Preparation and characterization of nanostructured powders of hydroxyapatite

Martínez-Castañón G. A. [*], Loyola-Rodríguez J. P., Zavala-Alonso N. V.
Maestría en Ciencias Odontológicas, Facultad de Estomatología, UASLP
Av. Manuel Nava No. 2, Zona Universitaria, San Luis Potosí, S. L. P., México

Hernández-Martínez S. E.
Maestría en Metalurgia e Ingeniería de Materiales, Facultad de Ingeniería, UASLP
Av. Manuel Nava No. 2, Zona Universitaria, San Luis Potosí, S. L. P., México

Niño-Martínez N., Ortega-Zarzosa G.
[a]Facultad de Ciencias, UASLP
Álvaro Obregón No. 64, Col. Centro, San Luis Potosí, S. L. P., México

Ruiz F.[a]
Centro de Investigación en Materiales Avanzados, Alianza Norte No. 202, Parque de Investigación e Innovación Tecnológica, Apodaca, Nuevo León, México
(Recibido: 15 de diciembre de 2011; Aceptado: 13 de mayo de 2012)

In this work, hydroxyapatite nanostructured powders were prepared with different crystallinity degree, crystal size and morphology using a simple aqueous precipitation method varying the pH and temperature parameters. We found that at higher pH values the crystal size grows and crystallinity was improved; at higher temperatures there is also a crystal size growth and crystallinity improving but this change is more significant, a change in the morphology of the nanopowders was also observed. Using XRD patterns and Rietveld analysis we found that the crystal size change from 9.15 to 26.4 nm. The prepared powders are highly agglomerated with a pseudo-spherical and rod-like morphology.

Keywords: Hydroxyapatite; Precipitation; Chemical synthesis; Nanopowders

1. Introduction

Hydroxyapatite (HA) [$Ca_{10}(PO_4)_6(OH)_2$] is the major inorganic component of biological hard tissues, on its synthetic form, HA can be used as coating in orthopedic and dental implants [1], chromatography for proteins [1,2] replacement for hard tissues, adsorbents for nucleic acids, fillers [3] gene silencing and transfection [4]. The properties and applications of synthetic HA are strongly influenced by its crystallinity, composition, crystal size and agglomeration and it is expected that nanocrystalline HA present a better bioactivity than coarser crystals [2, 5, 6]. In medical and dental fields, the major application of this material is as bone graft, where HA is used to promote the growth of new bone. The successful growth of new bone tissue requires HA being biodegradable and bioresorbable, these characteristics are influenced by crystal size and crystallinity; the solubility of hydroxyapatite increases from crystalline to amorphous and a reduction in crystal size also increases the solubility rate. Different application requires materials with different resorption rates, and then it is very important to develop a method that controls these properties from the synthesis of the material. HA can be prepared by different methods as solid state reaction, sol-gel, molten salts, liquid-solid solution, electrochemical deposition, hydrothermal technique, hydrolysis and precipitation [5]. Chemical precipitation in aqueous solution is one of the most used techniques due to its relative simplicity and low cost with a high yielding of products [7]. In this work, we have prepared calcium-deficient hydroxyapatite (CDHA) nanostructured powders with different crystallinity degree, different crystal size and different morphologies using a simple aqueous precipitation method varying the pH and temperature parameters in order to obtain a material with different and controllable biodegradation and bioabsorption characteristics (which will be further investigated) that could be used in several applications in dental and medical fields.

2. Materials and Methods

2.1 Synthesis of CDHA nanopowders

For a typical procedure, 100 mL of a 0.5 M calcium chloride ($CaCl_2$, 99.99%, Sigma Aldrich) solution was placed in a reactor vessel. Under magnetic stirring and once the temperature and pH were modified (see Table 1 for details) 100 mL of a 0.3 M ammonium hydrogenphosphate ($(NH_4)_2HPO_4$, 99.99%, Sigma Aldrich) solution was added at 2 mL/min using a peristaltic pump. The pH of the solution was modified and maintained using a 0.1 M NH_4OH solution. After the $(NH_4)_2HPO_4$ solution was completely added, the obtained material was filtered, washed two times with deionized water (in order to remove unreacted ions and subproducts), two times with acetone

[*] mtzcastanon@fciencias.uaslp.mx

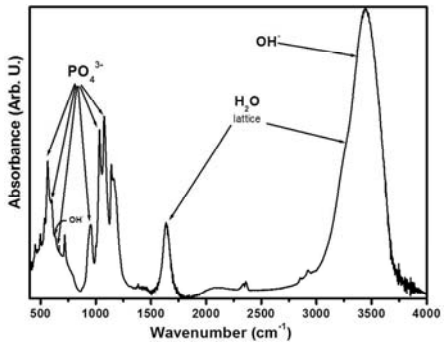

Figure 1. Infrared spectra for sample HA6.

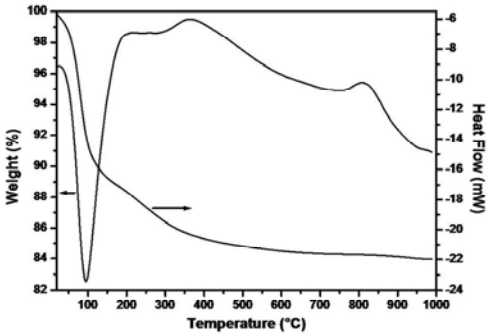

Figure 2. DCS analysis for sample HA1.

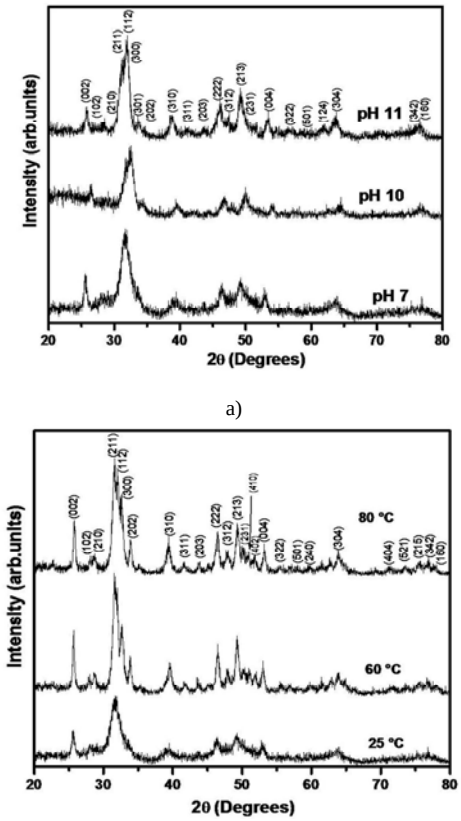

Figure 3. X ray diffraction patterns of the six samples prepared in this work. a) Samples prepared at different pH values at 25 °C, b) Samples prepared at different temperatures at pH=7. For details see Table 1.

and finally dried under ambient conditions. Five samples were thus obtained; named HA1, HA2, HA3, HA5 and HA6 (see Table 1 for details).

2.2 Characterization

The obtained dried powders were characterized using Differential Scanning Calorimetry (DSC) in a DSC 500 calorimeter from Waters using a constant heating rate of 2 °C/min from room temperature to 1000 °C; X-Ray Diffraction (XRD) patterns were obtained on a GBC-Difftech MMA model, with a Cu K_a irradiation at l= 1.54 Å; SEM micrographs were obtained using the secondary electrons detector in an Scanning Electron Microscope (SEM) Phillips XL-30. Transmission Electron Microscopy (TEM) analysis was performed on a JEOL JEM-1230 at an accelerating voltage of 100 kV. The infrared (IR) spectra were recorded in a FT-IR spectrometer Nicolet system model Avatar using the diffuse reflectance (DR) mode.

DSC and XRD analysis were performed using the as-prepared powders after drying under atmospheric conditions. Samples for SEM observation were prepared by dispersing the powders in ethanol and immersing them in an ultrasonic bath for 5 min, few drops of the resulting suspension were placed onto a SEM specimen mount, dried in air and gold coated. Samples for TEM analysis were prepared by dispersing the powders in ethanol and immersing them in an ultrasonic bath for 5 min, few drops of the resulting suspension were placed onto a Formvar coated copper grid. Infrared (IR) absorption spectra were taken by the KBr method, for which 0.05 g of powder sample were mixed with 0.3 g of KBr.

3. Results and Discussion

Figure 1 shows infrared spectra obtained from the as prepared sample HA6, bands at 560-650 cm^{-1} and 950-1100 cm^{-1} can be assigned to PO_4^{3-} group; signals at 560, 575 and 600 cm^{-1} correspond to phosphate ions in apatitic environments, signals at 617 and 634 cm^{-1} correspond to phosphate ions in non-apatitic environments; bands at 632 and 3570 cm^{-1} can be assigned to the OH^- group; bands at 1635 and 3440 cm^{-1} can be assigned to lattice water molecules in HA powders present as an structured hydrated surface layer [2, 11, 12]. According to Rey et al. [12] a non-apatitic environment could be a calcium-deficient or an amorphous environment. The position of the bands present in this infrared spectrum agrees well with those reported by several authors for pure HA [12, 13, 17].

Figure 2 shows DSC results from the thermal analysis made to sample HA1 (the rest of the samples present similar features, that is, the changes made to the synthesis method do not change the thermal behavior of the samples), we can see an endothermic peak at 95 °C which corresponds to the desorption of water molecules and is accompanied by a weight loss of approximately 15 wt%, this result agrees with those reported by Mobasherpour et al. [6] and Urch et al. [8], they prepared calcium phosphate nanoparticles in the form of HA, using a chemical

precipitation method, with a similar water content. As already mentioned, this water content could be present as an structured hydrated surface layer which is a very desirable condition due to its rol in the surface reactivity and in the maturation process of hydroxyapatite powders [12]. We can also see two exothermic peaks at 363 and 813 °C; the first one could be due to a crystallization process of the powder; the second one can be assigned to the decomposition of CDHA into β-tricalcium phosphate. This decomposition was further investigated by annealing sample HA1 at 900 ºC during 1 hour; the annealed powder was analyzed using X-ray diffraction and Rietveld analysis and we found that the fraction of the β-tricalcium phosphate in the final product was 13 %wt. The decomposition of HA powders into β-tricalcium phosphate is a characteristic of Ca-Deficient HA powders [1, 5, 18].

One of the main characteristics of HA is its bioabsorption which is directly related to crystal size and crystallinity [10]. Figure 3 shows XRD results of the CDHA nanopowders prepared, the five samples can be indexed as hexagonal hydroxyapatite as compared with JCPDS card no. 09-0432 and no other phases or compounds can be detected indicating that the prepared samples are pure HA, these results disagree with those reported by Li et al. [16], they obtained different phases at different pH values, the differences among both investigations are that they use ethanolamine, PEG-1200 or citric acid as dispersant in either water or a water-ethanol mixture. As we can see in Figure 3a, at higher pH values diffraction peaks are more defined, probably as a consequence of a higher crystallinity degree promoted by the presence of OH^- groups as explained by Kim et al. [11]. According to Kim, a low concentration of OH^- groups limits the crystallization of hydroxyapatite leaving a fraction of the material in the amorphous state.

A significant change in the resolution of the diffraction peaks was promoted by changing the reaction temperature from 25 to either 60 or 80 °C (Figure 3b). Diffraction pattern of the sample prepared at 25 ºC presents very broad peaks as a consequence of either a poor crystallinity or a very small crystal size, peaks of the samples prepared at 60

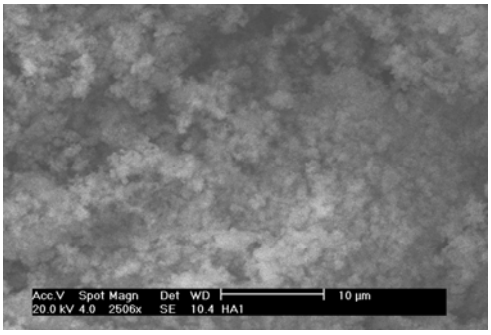

a)

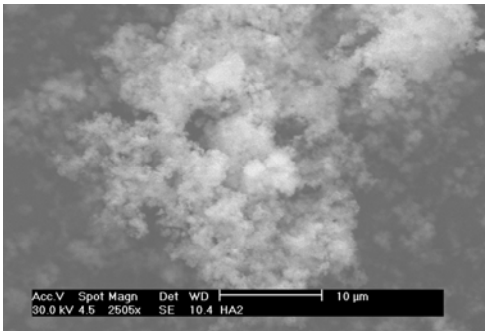

b)

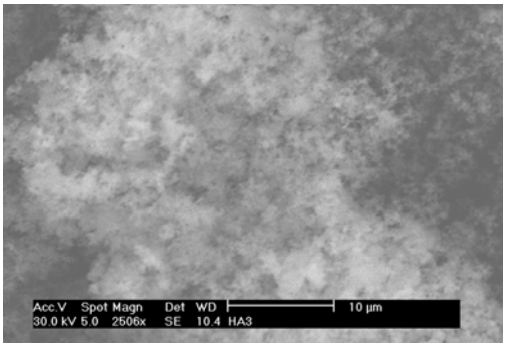

c)

Figure 4. SEM images of samples prepared at different pH values. a) Sample HA1, b) Sample HA2 and c) Sample HA3. See Table 1 for details.

Table 1. Reaction conditions, crystal size and lattice parameters of the samples prepared in this work.

	Synthesis conditions			Lattice Parameters	
Sample label	**pH**[a]	**Temperature** (°C)	**Crystal size**[b] (nm)	**a**[b] (Å)	**c**[b] (Å)
HA1	7.0	25	9.15	9.47534	6.88520
HA2	10.0	25	10.12	9.55656	6.81409
HA3	11.0	25	16.68	9.58103	6.82260
HA5	7.0	60	25.56	9.43544	6.88774
HA6	7.0	80	26.40	9.48253	6.87898

[a]This pH value was maintained until the reaction was completed with a variation of ± 0.01
[b]Calculated using diffraction patterns and Rietveld analysis

or 80 ºC are more defined and resolved. Due to the very low size of the crystallites it is rather than difficult to determine the individual contribution of the particle size and the poor crystallinity to the broadening of the diffraction patterns [5].

Crystal size and lattice parameters for every sample were calculated using Rietveld analysis using the MAUD software. The program MAUD was developed to analyze diffraction patterns and obtain crystal structures, quantity, and microstructure of phases along with the texture and residual stresses. It applies the RITA/RISTA method as developed by Wenk et al. [12] and Ferrari and Lutterotti [13].

As we can see in Table 1, crystal size grows either raising the pH or temperature values, this growth in crystal size could also be the responsible of the better definition of the diffraction peaks at the different pH and temperatures.

These results agree well with those reported by Rey et al. [12] and Drouet et al. [13], they report an increase in crystal size and crystallinity at higher temperatures and pH values.

Lattice parameters, calculated from Rietveld analysis, are reported in Table 1; all experimental parameters are different from those reported as standard values (a=b=9.4160 and c=6.8830 Å), the sample with the closest values was HA5 (prepared at pH=7 and 60 ºC).

Figure 4 shows SEM images of samples HA1, HA2 and HA3. The powders are highly agglomerated and present a pseudospherical morphology; in this case, variations in pH values do not influence the morphology and agglomeration of the powders. Samples HA1, HA5 and HA6 were observed using TEM. From Figure 5 we can see an increment in the size of the HA nanopowders as a consequence of the increment in the synthesis temperature, but the most significant change can be found in the morphology of the particles; sample prepared at 25 ºC present**s** an irregular morphology and particle size about 10-20 nm (Figure 5a), samples prepared at 60 and 80 ºC present a rod-like morphology with sizes about 20 nm in the short axis and 100-200 nm in the long axis (Figures 5b and 5c), having a greater aspect ratio the particles prepared at 80 ºC. Changes in morphology could be a consequence of changes in solubility of the starting reagents at the synthesis temperatures used in this work. The growth of hydroxyapatite rods usually occurs along the c-axis [2], in our samples this growth is reflected as an increment in the relative intensity of the peak assigned to (002) in Figure 3b, relative intensities for (002) signal for samples HA1, HA5 and HA6 are 51.72, 70.51 and 79.86 respectively. A probable mechanism for the formation of this HA rods could be Ostwald ripening, as we can see in Figure 5d (a magnification of sample HA6) rods are formed by smaller particles with sizes around 5 nm.

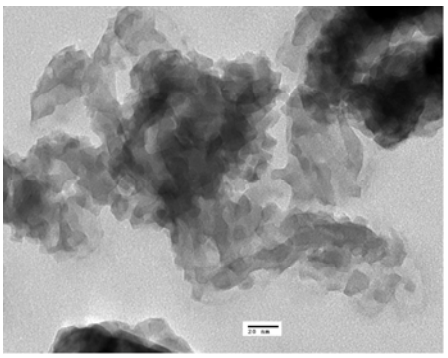

a)

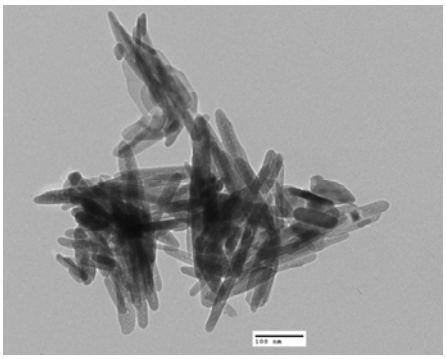

b)

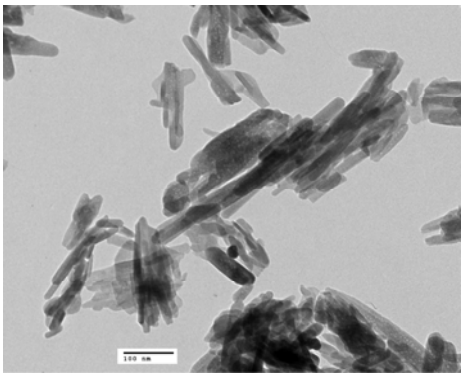

c)

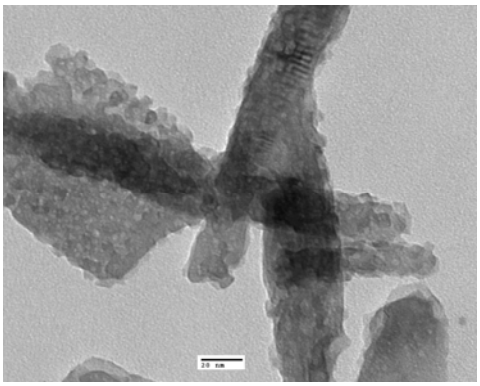

d)

Figure 5. TEM images of samples prepared at different temperature values. a) Sample HA1, b) Sample HA5, c) and d) Sample HA6. See Table 1 for details.

4. Conclusions

Ca-deficient hydroxyapatite nanostructured powders have been prepared using a simple templateless chemical precipitation method. The prepared powders present differences in cristallinity, crystal size and morphology as a consequence of changes on pH and temperature made in the synthesis method. It is rather than difficult to decide, at this point, the best synthesis conditions, but this investigation allow us to obtain different materials which differences can be related, in a further investigation, with their biodegradability and solubility and then we could decide the final clinical application of this material.

Acknowledgements

This work was partially supported by Consejo Nacional de Ciencia y Tecnología (CONACYT), Programa de Mejoramiento del Profesorado (PROMEP) and Fondo de Apoyo a la Investigación (FAI) of Universidad Autónoma de San Luis Potosí (UASLP).

References

[1]. S. V. Dorozhkin, M. Epple, Chem. Int. Ed. **41**, 3130 (2002).
[2]. I. S. Neira, Y. V. Kolen'ko, O. I. Lebedev, G. Van Tendeloo, H. S. Gupta, F. Guitián, M. Yoshimura, Cryst Growth Des. **9**, 466 (2009) .
[3]. Y. Liu, D. Hou, G. Wang, Mater Chem Phys. **86**, 69 (2004).
[4]. M. Epple, K. Ganesan, R. Heumann, J. Klesing, A. Kovtun, S. Neumann, V. Sokolava, J. Mater. Chem. **20**, 18 (2010).
[5]. S. V. Dorozhkin, Acta Biomaterialia. **6**, 715 (2010).
[6]. I. Mobasherpour, M. Soulati Heshajin, A. Kazemzadeh, M. Zakeri, J Alloy Compd. **430**, 330 (2007).
[7]. D. W. Kim, I. Cho, J. Y. Kim, H. L. Jang, G. S. Han, H. Ryu, H. Shin, H. S. Jun, H. Kim, K. S. Hong, Langmuir **26**, 384 (2010).
[8]. H. Urch, M. Vallet-Regi, L. Ruiz, J. M. Gonzalez-Calbet, M. Epple, J. Mater Chem. **19**, 2166 (2009).
[9]. W. Kim, Q. Zhang, F. Saito, J Mater Sci. **35**, 5401 (2000).
[10]. T. Welzel, W. Meyer-Zaika, M. Epple, Chem Commun.. 1204 (2004).
[11]. H. Kim, R. P. Camata, Y. K. Vohra, W. R. Lacefield, J Mater Sci-Mater M. **16**, 961 (2005).
[12]. C. Rey, C. Combes, C. Drouet, H. Sfihi, A. Barroug, Mater Sci Eng C. **27**, 198 (2007).
[13]. C. Drouet, F. Bosc, M. Banu, C. Largeot, C. Combes, G. Dechambre, C. Estournès, G. Raimbeaux, C. Rey, Powder Technol. **190**, 118 (2009).
[14]. H. R. Wenk, S. Matthies, L. Lutterotti, Materials Science Forum **157**, 473 (1994).
[15]. M. Ferrari, L. Lutterotti, J Appl Phys.**76**, 7246 (1994).
[16]. P. Wang, C. Li, H. Gong, X. Jiang, H. Wang, K. Li, Powder Technology. **203**, 315 (2010).
[17]. Y. Sakhno, L. Bertinetti, M. Iafisco, Anna Tampieri, Norberto Roveri, Gianmario Martra, J. Phys. Chem. C. **114**, 16640 (2010).
[18]. R. M. Wilsona, J. C. Elliotta, S. E. P. Dowkerb, L. M. Rodriguez-Lorenzo, Biomaterials. 26, 1317 (2005).